DMD Fast Forward. Published on February 2, 2018 as DOI: 10.1124/dmd.117.078915
This article has not been copyedited and formatted. The final version may differ from this version.

Title Page:

Mathematical and experimental validation of flux dialysis method: An improved approach to measure unbound fraction for compounds with high protein binding and other challenging properties

J. Cory Kalvass, Colin Phipps, Gary J. Jenkins, Patricia Stuart, Xiaomei Zhang, Lance Heinle Marjoleen J.M.A. Nijsen and Volker Fischer

Drug Metabolism, Pharmacokinetics and Bioanalysis, Research & Development, AbbVie, North Chicago, IL 60064

Running title page:

Running title: Determination of unbound fraction by flux dialysis method

Corresponding author:

J. Cory Kalvass

AbbVie Inc.

1 North Waukegan Road,

North Chicago, IL 60064-6104, USA

Phone: (847) 937-8987

Email: j.kalvass@abbvie.com

Number of text pages: 33

Number of tables: 4

Number of figures: 5

Number of references: 25

Number words in the Abstract: 249

Number words in the Introduction: 767

Number words in the Discussion: 1873

Non-standard abbreviations: A, dialysis membrane surface-area; C, compound concentration; D, matrix dilution factor; f_u, unbound fraction; HPLC, high performance liquid chromatography; k_{loss}, compound first-order rate of irreversible loss; K_{nsb}, binding potential (B_{max}/K_D); LLOQ, lower limit of quantification; MS/MS, tandem mass spectrometry; MWCO, molecular weight cutoff; P_{mem}, compound unbound dialysis membrane permeability; R, receiver/donor concentration ratio; R_{eq}, receiver/donor concentration ratio at steady-state equilibrium; R_{slope}, derivative of concentration ratio with respect to time (dR/dt) under initial sink conditions; SF, scaling factor; $t_{1/2,eq}$, dialysis equilibration half-life; V, compartment-volume; X_0, compound mass at time zero

Abstract:

A flux dialysis method to measure unbound fraction (f_u) of compounds with high protein binding and other challenging properties was tested and validated. The method is based on the principle that the initial flux rate of a compound through a size-excluding dialysis membrane is proportional to the product of compound initial concentration, f_u and unbound dialysis membrane permeability (P_{mem}). Therefore f_u can be determined from initial concentration and flux rate, assuming membrane P_{mem} is known. Compound initial flux rates for 14 compounds were determined by dialyzing human plasma containing compound (donor side) versus compound-free plasma (receiver side) and measuring the rate of compound appearance into the receiver side. Eleven compounds had known f_u values obtained from conventional methods (ranging from 0.000013 to 0.22) while three compounds (bedaquiline, lapatinib, and pibrentasvir) had previously qualified f_u values (e.g., < 0.001). P_{mem} estimated from flux rates and known f_u values did not meaningfully differ among compounds and were consistent with previously published values, indicating that P_{mem} is a constant for the dialysis membrane. This P_{mem} constant and the individual compound flux rates were used to calculate f_u values. The flux dialysis f_u values for the 11 compounds were in good agreement with their reported f_u values (all within 2.5-fold; R^2=0.980) confirming the validity of the method. Furthermore, the flux dialysis method allowed discrete f_u to be estimated for the 3 compounds with previously qualified f_u. Theoretical and experimental advantages of the flux dialysis method over other dialysis-based protein binding methods are discussed.

DMD Fast Forward. Published on February 2, 2018 as DOI: 10.1124/dmd.117.078915
This article has not been copyedited and formatted. The final version may differ from this version.

Introduction:

Determination of the unbound fraction (f_u) of a compound is essential for the interpretation of disposition, efficacy (i.e., free drug exposure at the pharmacological target), drug-drug interaction, and safety data. While many different methodologies (ultrafiltration, ultracentrifugation, equilibrium gel filtration, etc.) have been utilized to measure compound f_u from biological matrices, equilibrium dialysis is one of the most commonly used approaches since it is inexpensive, easy to perform, automatable and reliable for most compounds (Di et al, 2015). However, accurate f_u values can only be determined by equilibrium dialysis when equilibrium is truly achieved, compound and matrix do not degrade during the time-course of dialysis, and the buffer unbound concentration is above the bioanalytical lower limit of quantification (LLOQ). Several dialysis-based alternative approaches (e.g., plasma vs plasma competition, plasma dilution and pre-saturation methods) which attempt to address some of these challenges have been proposed and recently reviewed in literature (Clarke et al., 2008; Di et al., 2012; Riccardi et al., 2015), but the need to reach equilibrium, low compound concentrations on the receiver side and the liabilities of non-specific binding still exist. Interestingly, an infrequently used dialysis approach, dynamic dialysis, first developed in the 1950s has the capability of measuring much lower f_u values than equilibrium dialysis and has the potential to address these challenges. With this approach, compound-spiked serum is dialyzed against compound-free serum and the relative f_u of compound is determined from the initial slope of compound appearance in the receiver compartment, using the principle that the compound's relative permeability across the dialysis membrane is proportional to the compound's relative f_u (Christensen, 1959). The absolute f_u of a compound may be determined in a similar manner if a compound's unbound dialysis membrane permeability (P_{mem}) is known (Meyer and Guttman,

1968; Meyer and Guttman, 1970a; Meyer and Guttman, 1970b; Ross, 1978). Measuring a compound's f_u with the dynamic dialysis method offers advantages over equilibrium dialysis, namely allowing much higher receiver concentration to be achieved (enabling measurements of lower f_u values for a given LLOQ) and reducing non-specific binding to the dialysis device (Ross, 1978). Despite these advantages, dynamic dialysis is rarely used compared to equilibrium dialysis. During the 1950s-70s when dynamic dialysis methods were primarily being developed and used, they likely suffered from the following disadvantages compared to equilibrium dialysis:

1. A higher level of radiochemical purity was required since dynamic dialysis methods are highly susceptible to experimental artifacts introduced by radiochemical impurities (Christensen, 1959).

2. Multiple time-points needed for dynamic dialysis decreased experimental throughput and increased workload compared to single time-point equilibrium dialysis. This was especially true considering the available technology of the time (e.g., large individual closed-cell dialysis units, bioanalytical methods with long run times often requiring extensive sample extraction or cleanup).

3. Dynamic dialysis method required measurement of P_{mem} for each compound, which could be laborious and challenging for compounds exhibiting high non-specific binding (Meyer and Guttman, 1970a).

We reasoned that these disadvantages could be mitigated by modern technology (improved bioanalytical methodologies, mass spectrometry, high-throughput 96-well equilibrium dialysis devices, kinetic modeling, etc.) and sought to test and validate a new modern dynamic dialysis approach (*flux dialysis*) as an improved way to measure f_u for compounds with high protein

DMD Fast Forward. Published on February 2, 2018 as DOI: 10.1124/dmd.117.078915
This article has not been copyedited and formatted. The final version may differ from this version.

binding and other challenging properties. To explore the intrinsic differences between flux dialysis and other dialysis-based methods, a dialysis kinetic model was built. The model describes the time-course of compound concentrations in the donor and receiver compartments during dialysis, accounting for both compound degradation and device non-specific binding. The utility and applicability of the flux dialysis approach was further investigated by using a test set of 14 compounds with reported human plasma f_u values covering four orders of magnitude (0.000013 – 0.22) and diverse physicochemical properties (mol. wt. 280 – 1113; cLogP -0.88 – 8.1; polar-surface-area 6.5 – 204 A^2 ; intrinsic solubility 0.003 – 450 μM). Three of the test set compounds (bedaquiline, lapatinib and pibrentasvir) have extremely high plasma protein binding values such that only qualified f_u values have been reported using conventional protein binding methods. Two other compounds, UCN-01 and venetoclax, were selected for inclusion in the test set because discrete f_u values could only be measured using diluted plasma and in addition UCN-01 demonstrated saturable plasma protein binding. A detailed analysis of UCN-01 and venetoclax f_u values determined from diluted plasma (using conventional and/or flux dialysis) and undiluted plasma (using flux dialysis) was conducted. Accuracy, precision, and sensitivity of f_u measurements determined from the flux dialysis method were compared to reported f_u results determined from other methods. Theoretical and experimental advantages of the flux dialysis method are discussed in the context of other dialysis-based protein binding methods.

DMD Fast Forward. Published on February 2, 2018 as DOI: 10.1124/dmd.117.078915
This article has not been copyedited and formatted. The final version may differ from this version.

Materials and Methods:

Materials

Human plasma was purchased from Bioreclamation IVT (Hicksville New York); typical lots consisted of a pool from 25 male donors. Test compounds (amiodarone, bedaquiline, glecaprevir, glyburide, indomethacin, imipramine, itraconazole, lapatinib, nelfinavir, pibrentasvir, quinidine, sertraline, and venetoclax) were obtained from the Global Compound Logistics and Operations Department at AbbVie, Inc (Lake County, Illinois). UCN-01 was obtained from Sigma-Aldrich (catalog# U6508-5MG). The 96-well equilibrium dialysis device (HTD-96b, high-throughput dialysis device in a 96-well format) and cellulose membranes with weight cut-off (MWCO) of 12-14 KD were purchased from HT-Dialysis (Gales Ferry, Connecticut). Breathe Easy^{TM} gas permeable adhesive seals were obtained from Sigma-Aldrich (St. Louis, Missouri). Deep well plates were from Analytical Sales and Service (Flanders, New Jersey). Sodium azide was obtained from Sigma-Aldrich (catalog# S2002-5G).

Dialysis Kinetic Modeling and Derivation for Flux Dialysis Methodology

A two compartment kinetic model describing the time-course of compound donor and receiver concentrations during dialysis was constructed (Figure 1). The model structure was general, allowing consideration of dialysis between any two matrices (e.g., plasma vs buffer, buffer vs buffer, plasma vs plasma). Kinetic relationships revealed that under initial sink conditions (i.e., donor matrix concentration ≈ initial concentration, and receiver unbound << donor unbound matrix concentration), the rate of compound appearance into receiver compartment (i.e., flux) is directly proportional to donor matrix unbound fraction ($f_{u,donor}$). Mathematical relationships between the f_u values in donor and receiver matrices ($f_{u,donor}$ and $f_{u,receiver}$), compound unbound

DMD Fast Forward. Published on February 2, 2018 as DOI: 10.1124/dmd.117.078915
This article has not been copyedited and formatted. The final version may differ from this version.

dialysis-membrane permeability (P_{mem}), dialysis-membrane area (A), receiver/donor compound concentration ratio (R), compartment volumes (V) and initial flux rate (R_{slope}) were formulated. The resulting relationships provided a mathematical basis to calculate $f_{u,donor}$ and $f_{u,receiver}$ from receiver/donor concentration ratio data obtained from dialysis experiments. An abbreviated description of the kinetic model is presented here, however, an expanded derivation accounting for the influence of non-specific binding and compound degradation is presented and solved in Appendix A.

The dialysis kinetic model (Figure 1) is comprised of a donor matrix and a receiver matrix compartment separated by a semipermeable membrane. Assuming negligible non-specific binding to device and negligible compound degradation, the differential equations for donor and receiver concentrations are given by:

$$V_{donor}\frac{dC_{donor}}{dt} = (P_{mem} \times A)\left(f_{u,receiver} \times C_{receiver} - f_{u,donor} \times C_{donor}\right) \quad \text{Eq. (1)}$$

$$V_{receiver}\frac{dC_{receiver}}{dt} = (P_{mem} \times A)\left(f_{u,donor} \times C_{donor} - f_{u,receiver} \times C_{receiver}\right) \quad \text{Eq. (2)}$$

The initial conditions are $C_{donor} = X_0/V_{donor}$ and $C_{receiver} = 0$, where X_0 is the amount of compound in the donor compartment at time = 0. At equilibrium the system reaches a steady state where $f_{u,receiver} \times C_{receiver} = f_{u,donor} \times C_{donor}$ and therefore $\frac{C_{receiver}}{C_{donor}} = \frac{f_{u,donor}}{f_{u,receiver}}$. The concentration ratio as a function of time is denoted as $R = \frac{C_{receiver}}{C_{donor}}$; and the steady-state concentration ratio is denoted as $R_{eq} = \frac{f_{u,donor}}{f_{u,receiver}}$.

DMD Fast Forward. Published on February 2, 2018 as DOI: 10.1124/dmd.117.078915
This article has not been copyedited and formatted. The final version may differ from this version.

There is no loss in this model, so mass is conserved and satisfies the relationship $(C_{receiver} \times V_{receiver}) + (C_{donor} \times V_{donor}) = X_0$, at all times.

Under initial sink conditions the following conditions are held:

$V_{donor} \frac{dC_{donor}}{dt} = 0$; $C_{donor} = {X_0}/{V_{donor}}$; and $f_{u,receiver} \times C_{receiver} \ll f_{u,donor} \times C_{donor}$

Solving for compound flux rate into the receiver compartment under these sink conditions yields:

$$flux = V_{receiver} \times \frac{dC_{receiver}}{dt} = f_{u,donor} \times C_{donor} \times P_{mem} \times A \qquad \text{Eq. (3)}$$

Eq. (3) indicates initial rate of compound appearance into receiver compartment (i.e., flux) is directly proportional to $f_{u,donor}$.

Since the donor concentration is approximately constant under initial sink conditions, the initial flux rate in Eq. (3) can be rearranged to yield the approximation at time=0:

$$\frac{dR}{dt} = \frac{f_{u,donor} \times P_{mem} \times A}{V_{receiver}} \qquad \text{Eq. (4A)}$$

From Eq. (4A), the initial rate of change in receiver/donor concentration ratio under initial sink conditions is directly proportional to $f_{u,donor}$. This initial slope is denoted by

$$R_{slope} = \frac{f_{u,donor} \times P_{mem} \times A}{V_{receiver}}. \qquad \text{Eq. (4B)}$$

If these initial sink conditions are met, then R_{slope} can be approximated from R versus time data by linearly fitting the initial slope from one or more early time-points.

Alternatively, R_{slope} can be approximated from R versus time data by fitting the exponential Eq. (5) to the data and then solving for R_{slope} according to Eq. (6) where k is the exponential rate constant and R_{eq} is the steady state concentration ratio as previously defined.

$$R = R_{eq} \times \left(1 - e^{-k \times t}\right) \quad \text{Eq. (5)}$$

$$R_{slope} = R_{eq} \times k \quad \text{Eq. (6)}$$

Approximating R_{slope} using exponential Eq. (5) and (6), allows data from the entire time-course to be used without needing to decide which time-points to include or exclude from the initial slope and simultaneously provides an estimate for R_{eq}. Moreover, this approach allows R_{slope} to be estimated even if early time-points from the initial slope are missing.

In the cases where it is warranted to estimate R_{slope} from a single time-point, Eq. (5) and (6) can be solve for R_{slope} which gives

$$R_{slope} = \frac{R_{eq} \times \ln\left(\frac{R_{eq}}{R_{eq} - R}\right)}{t} \quad \text{Eq. (7)}$$

Using Eq. (7) to estimate R_{slope} from a single time-point does not require the time-point to be taken during initial sink conditions, therefore is more accurate and preferable to estimating R_{slope} from the slope between the single time-point and zero, which *does* require the time-point to be taken during initial sink conditions. However, if two or more time-points are available then

DMD Fast Forward. Published on February 2, 2018 as DOI: 10.1124/dmd.117.078915
This article has not been copyedited and formatted. The final version may differ from this version.

fitting exponential Eq. (5) to the data is more accurate and preferable over using single time-point and Eq. (7) since R_{slope} is estimated from the totality of data rather than using a single time-point.

The application of these equations and theory will be described below.

Flux dialysis data were analyzed by fitting Eq. (5) to receiver/donor concentration ratio (R) versus time data using Phoenix 64 Build 6.3.0.395 non-linear regression software with 1/y weighting. R_{slope}, which equals dR/dt at t=0, was calculated from either Eq. (6) or (7). R_{eq}, the equilibrium receiver/donor concentration ratio, was fixed to 1 since both receiver and donor matrix were composed of identical plasma.

If R_{slope} and R_{eq} are estimated from flux dialysis data and the device parameters $A/V_{receiver}$ and P_{mem} are known then $f_{u,donor}$ and $f_{u,receiver}$ can be estimated by a rearrangement of Eq. (4B) and the definition of R_{eq} as given below in Eq. (8) and (9).

$$f_{u,donor} = \frac{V_{receiver}}{P_{mem} \times A} \times R_{slope} \qquad \text{Eq. (8)}$$

$$f_{u,receiver} = \frac{f_{u,donor}}{R_{eq}} \qquad \text{Eq. (9)}$$

Here we have assumed that P_{mem} is a device-specific parameter that is constant across compounds. The validity and impact of this assumption will be addressed below. The device-specific proportionality constant between $fu_{,donor}$ and R_{slope} given in Eq. (8) is a scaling factor (SF) that can be used to translate between the calculated R_{slope} value and the desired estimate of

f_u. Denoting this strictly device-dependent scaling factor by SF, where $SF = \frac{V_{receiver}}{P_{mem} \times A}$, yields the simplified version of Eq. (8)

$$f_{u,donor} = SF \times R_{slope}. \quad \text{Eq. (10)}$$

If $A/V_{receiver}$ or P_{mem} of the dialysis device is unknown, then SF must first be estimated before utilizing Eq. (10). In this case SF can be determined by the R_{slope} and f_u from one or more reference compounds, denoted by $R_{slope,ref}$ and $f_{u,ref}$ respectively. Rearranging Eq. (10) for a reference compound gives

$$SF = \frac{f_{u,ref}}{R_{slope,ref}} \quad \text{Eq. (11)}$$

indicating that the ratio of f_u to R_{slope} is constant and equal to SF. SF can then be estimated from this ratio in Eq. (11) for one reference compound or from the average SF values calculated for multiple reference compounds. The latter approach could reduce experimental variability or error in determining SF from a single compound R_{slope} and $f_{u,ref}$ value. This estimated SF, along with a measured value of R_{slope} can then be used in Eq. (10) to yield specific estimates of $f_{u,donor}$.

For the dialysis device used in this study, the membrane surface area-to-volume ratio ($A/V_{receiver}$) provided by the manufacturer was 3.7 cm^2/mL (Banker et al., 2003) while the P_{mem} constant was unknown. The SF value was calculated for each reference compound and the corresponding P_{mem} was calculated from a rearrangement of the definition of SF:

DMD Fast Forward. Published on February 2, 2018 as DOI: 10.1124/dmd.117.078915
This article has not been copyedited and formatted. The final version may differ from this version.

$$P_{mem} = \frac{1}{SF} \times \frac{V_{receiver}}{A} = \frac{1}{SF} \times \frac{1}{3.7\ cm^2/mL} \quad \text{Eq. (12)}$$

The average P_{mem} value constant was found to be 75.2×10^{-6} cm/s. Given the device $A/V_{receiver}$ ratio (3.7 cm^2/mL), this yields an equivalent value of SF=3590 s. Flux dialysis f_u was calculated according to Eq. (8) using this SF value, and each compound's average R_{slope}, giving the relationship

$$f_{u,donor} = (3590\ s) \times R_{slope}. \quad \text{Eq. (13)}$$

F_u values from diluted plasma ($f_{u,measured}$) were converted to undiluted f_u estimates using the equation

$$\text{Undiluted } f_u = \frac{1/D}{\left(1/f_{u,measured}\text{-}1\right)+1/D} \quad \text{Eq. (14)}$$

where D is the plasma dilution factor (Kalvass and Maurer, 2002).

Compound recovery from dialysis device was calculated from Eq. (15).

$$\text{Recovery (\%)} = \frac{C_{donor}+C_{reciever}}{C_{donor}\text{ at time equal zero}} \quad \text{Eq. (15)}$$

UCN-01 2-site binding parameters (1-site saturable, 1-site non-saturable) were calculated from flux dialysis f_u values determine at different UCN-01 concentrations (C) and plasma dilutions (D) according to the equation

$$f_u = \frac{C-\left(\frac{B_{max}}{D}+K_D\left(1+\frac{K_{nsb}}{D}\right)\right)+\sqrt{\left(C-\left(\frac{B_{max}}{D}+K_D\left(1+\frac{K_{nsb}}{D}\right)\right)\right)^2+4K_D\left(1+\frac{K_{nsb}}{D}\right)C}}{2\left(1+\frac{K_{nsb}}{D}\right)C} \quad \text{Eq. (16)}$$

DMD Fast Forward. Published on February 2, 2018 as DOI: 10.1124/dmd.117.078915
This article has not been copyedited and formatted. The final version may differ from this version.

where B_{max} is the saturable binding-site total concentration, K_D is the saturable binding-site equilibrium dissociation constant, K_{nsb} is the non-saturable binding-site binding potential ($B_{max,NS}/K_{D,NS}$), and D is the matrix dilution factor. Derivation of this 2-site saturable binding equation (1-site saturable, 1-site non-saturable) is presented in Appendix B.

Flux Dialysis Experiment

Flux dialysis experiments were conducted using a modification of a generalized equilibrium dialysis method from the literature (Kalvass et al., 2007). Regenerated cellulose membrane preparation (MWCO 12-14 KDa) and 96-well HTDialysis apparatus setup were consistent with the manufacturer's recommendations. Human plasma was supplemented with 10 μM sodium azide (final concentration) prior to use to prevent microbial growth over the long incubation period. Plasma containing 1 μM of test compound (donor matrix) was dialyzed against compound-free human plasma (receiver matrix) in the HTDialysis apparatus at 37°C in a 5% CO_2 atmosphere with shaking at 150 rpm for up to 120 hours. Aliquots (10 μL) of both receiver and donor matrix were taken at approximately 0, 0.25, 0.5, 2, 4, 24, 48, 96, 120 hours. Aliquots were frozen, for a minimum of 24 hours prior to analysis. Standard curve samples were prepared in human plasma containing 10 μM sodium azide to match dialysis samples. Additional flux dialysis studies using the same methodology were conducted with UCN-01 at 0.3, 1, 2, 3, 10, 30, 100 μM in undiluted plasma and 2 μM in plasma diluted 5-, 10-, and 20-fold.

Dilution-Method Equilibrium Dialysis Experiment for Venetoclax

The unbound fraction of venetoclax in human plasma was determined by equilibrium dialysis using a 96-well HTDialysis apparatus with dialysis membrane strips (MWCO 12-14 kDa). Venetoclax in 1% plasma was equilibrated against dialyzed phosphate buffer (50 mM, pH 7.4). Dialyzed buffer was prepared by dialyzing naïve human plasma with phosphate buffer (50 mM, pH 7.4) for 4 h at 37°C, mimicking a standard incubation but without the compound. Dialyzed buffer was prepared in advance and stored at -20°C until use. 1% dialyzed buffer was used on the receiver side with venetoclax in 1% plasma on the donor side. Dialyzed phosphate buffer was used during dialysis because low molecular weight plasma components (e.g., lipids, small peptides, nutrients, etc.) are pre-equilibrated with receiver buffer and are expected to help keep venetoclax in solution. After the incubation (4 h, 37°C), plasma (5 µL) and buffer (50 µL) were sampled from the dialysis plate and combined with acetonitrile/methanol containing 50 nM carbutamide as the internal standard (quench solution). The plasma samples were matrix blanked with buffer and the buffer samples were matrix blanked with plasma. Likewise, standard curve samples were matrix blanked to contain identical matrix composition as the dialysis samples. Samples were vortex-mixed and stored at 4°C, if necessary, prior to centrifugation and analysis by HPLC-MS/MS. The volumes of initial sampling (e.g., 5 µL plasma and 50 µL buffer) were taken into account during the quantitation of venetoclax, f_u values from diluted plasma ($f_{u,measured}$) were mathematically converted to values representing f_u in undiluted plasma using Eq. (14), where D is the plasma dilution factor (Kalvass and Maurer, 2002)

Flux Dialysis Sample Bioanalysis and Quantitation

Compound concentration in the matrix receiver and donor samples (e.g., human plasma) from the flux-dialysis time-course were quantitated using HPLC-MS/MS. Samples were quenched with a minimum of three volume equivalents of 95:5 acetonitrile: methanol containing 50 nM carbutamide (quench solution). Samples were vortex-mixed, centrifuged, and supernatant was injected for LC-MS/MS analysis. The HPLC-MS/MS method is summarized by the following. Ten microliters of sample were injected onto a Fortis Pace C18 column, using a CTC PAL autosampler, connected to an Agilent 1290 HPLC and an AB Sciex API-5500 Mass spectrometer with a turbo spray ion source. The sample was initially held at 95% of 0.1% formic acid (mobile phase A) and 5% of 0.1% formic acid in acetonitrile (mobile phase B) for 0.3 minutes. The gradient was ramped to 2% mobile phase A over the following 0.3 minutes, where it was held for an additional 0.4 minutes. The gradient was then brought back to initial conditions for 0.15 minutes. The total flow rate was held at 800 µL/min. The specific MS/MS setting used for each compound are listed in Table 1.

Peak areas for the compounds of interest were determined with Sciex Analyst™ 1.6 software. The mass spectrometer response for each sample containing the test article was compared to the mass spectrometer response from a set of standard concentrations prepared for the test article, using the Sciex Analyst™ 1.6 software. The concentration of each sample was then determined using the standard curves prepared in human plasma. The standard curves were fit using a quadratic 1/x weighted regression and met a minimum r-squared value of 0.98. The lower limit of quantitation was 1 nM for amiodarone, bedaquiline, glyburide, and lapatinib, 2 nM for imipramine, itraconazole, pibrentasvir, sertraline, UCN-01 and venetoclax, 10 nM for glecaprevir, and 20 nM for indomethacin, nelfinavir, and quinidine.

Results:

Dialysis Modeling Results

Relationships for the dialysis $C_{receiver}/C_{donor}$ time-course were solved for the model structure in Figure 1. Relationships for traditional equilibrium dialysis (matrix dialyzed against buffer) indicated nonspecific binding to device (i.e., $K_{nsb,device}$) has no impact on accurate f_u determination, as long as equilibrium has been achieved and k_{loss} is identical (or negligible) between matrix and buffer. In contrast, results for flux dialysis indicated obtainment of equilibrium is not required, and $K_{nsb,device}$ and k_{loss} have no influence on accurate f_u determination as long as binding affinity to the receiver matrix is greater than the nonspecific binding to device (i.e., $f_{u,receiver} << 1/ K_{nsb,device}$) and k_{loss} is identical (or negligible) between donor and receiver matrix, which is the case if identical matrix is used.

Dialysis equilibration half-life ($t_{1/2,eq}$), or time required to achieve 50% steady-state equilibrium between donor and receiver concentrations, for both flux dialysis and traditional equilibration dialysis conditions were solved (see Appendix A). Under flux dialysis conditions, assuming identical matrix composition on both sides and negligible device non-specific binding, $t_{1/2,eq}$ is inversely proportional to f_u. In contrast, under traditional equilibrium dialysis conditions, assuming negligible device non-specific binding, $t_{1/2,eq}$ is independent of f_u. The dialysis time to achieve equilibrium within the HTD-96b dialysis device was calculated as ~3.5 hours using derived relationship for $t_{1/2,eq}$ and assuming equilibration is achieved within ~5 equilibration half-lives (see Appendix A). In cases when device non-specific binding is not negligible, assuming

traditional equilibrium dialysis conditions, the time to reach equilibrium increases proportionally by the degree of non-specific binding or by a factor of $K_{nsb,device}$ +1.

The lowest measurable discrete f_u values from traditional equilibration dialysis (donor matrix dialyzed against buffer) and flux dialysis (identical donor and receiver matrix) were solved for as a function of bioanalytical sensitivity (i.e, LLOQ).

$$\text{equilibrium dialysis lowest discrete fu} = \sim \frac{\text{LLOQ}}{\text{C}_{\text{donor}}} \qquad \text{Eq. (17)}$$

$$\text{flux dialysis lowest discrete fu} = \sim \frac{\text{LLOQ}}{\text{C}_{\text{donor}}} \times \frac{V}{P_{mem} \times A} \times \frac{1}{t} \qquad \text{Eq. (18)}$$

The lowest discrete f_u from the flux dialysis method, substituting the P_{mem} constant (75.2×10^{-6} cm/s) and HTDialysis A/V ratio (3.7 cm^2/mL) was calculated as LLOQ/(C_{donor}×t) where t is expressed in hours. Comparison of non-specific binding, compound degradation, minimal dialysis time, and LLOQ considerations across 4 different dialysis-based protein binding approaches are summarized in Table 4.

Flux Dialysis Results

Using the flux dialysis method, all 14 compound receiver concentrations were above bioanalytical LLOQ at one or more time-points, allowing discrete R_{slope} value to be determined for each compound (Table 2). In contrast, the LLOQs achieved using AbbVie's default discovery bioanalytical method would have been insufficient to determine buffer concentrations for 8 of the 14 compounds from traditional equilibrium dialysis (plasma dialyzed against buffer), assuming 100% recovery. The flux dialysis receiver/donor matrix concentration ratio (R) versus time data were adequately described by $R=R_{eq}\cdot(1-e^{-k\cdot t})$ equation (Figure 2). R_{slope} values differed

by >10,000-fold among compounds (Table 2). R_{slope} estimates were obtained with a median inter-day %CV (95 percentile range) of 13% (2% - 32%) (Table 2).

The average P_{mem} constant (95% prediction interval) estimated from 11 compounds with known f_u was 75.2 (32 – 150) × 10^{-6} cm/s. All individual compound P_{mem} values were within 2.5-fold of the average value and no correlation between individual compound P_{mem} values and physiochemical properties (Table 3) were found indicating that any inaccuracy introduced by the assumption of constant P_{mem} is limited to this fold-error, which is within tolerated limits of in vitro assay variability.

Discrete f_u values from undiluted plasma and 1µM compound concentration were measurable for all 14 compounds using individual compound R_{slope} values and average P_{mem} constant. Flux dialysis f_u values differed more than 10,000-fold among compounds (0.14 – 0.000012). Flux dialysis f_u values were highly correlated with (r^2=0.980) and in good agreement (within ± 2.5-fold) with cited literature values obtained from other methods (Figure 3). All cited literature and flux dialysis f_u values were also similar (i.e., discrete f_u values within ~2-fold) to AbbVie historical equilibrium dialysis f_u values (data not shown; AbbVie historical f_u values were discrete for all compounds except for lapatinib, UCN-01, pibrentasvir, amiodarone, and bedaquiline for which only qualified f_u values could be determined).

Flux dialysis recovery for all compounds was ≥ 90%, except for indomethacin which declined mono-exponentially over time to ~20% by 120 hours (Figure 4A). Despite recovery of ~20%, the indomethacin flux time-course was fitted well by Eq. (5) (Figure 4B) and individual R_{slope} values estimated at each time-point using Eq. (7) were similar to the R_{slope} estimated from fitting entire time-course (Figure 4C). Indomethacin recovery was also ~20% from indomethacin

plasma control experiments incubated in 1.2 mL polypropylene tubes under identical conditions as the flux dialysis experiment. Indomethacin in vitro plasma half-life estimated from fitting exponential equation to the recovery time-course was 57±7 hours (Figure 4A).

UCN-01 Flux Dialysis Results

UCN-01 f_u values showed concentration dependent changes consistent with saturable protein binding (Figure 5). A novel mechanistic 2-site saturable binding equation (1-site saturable, 1-site non-saturable) was developed and fitted simultaneously to all UCN-01 flux dialysis f_u values generated under various experimental conditions. Estimates of B_{max}, K_D, and K_{nsb} obtained from fitting 2-site saturable binding equation were 10.1 μM, 0.00085 μM, and 21.2, respectively and matched closely (within 1.6-fold) those previously reported in the literature (16.4 μM, 0.0012 μM, and 20, respectively) determined using an ultracentrifugation method to measure UCN-01 binding to human plasma and alpha-1-acid glycoprotein (Fuse et al., 1998).

UCN-01 f_u values obtained at 2 μM concentration using 5-, 10-, and 20-fold diluted plasma exceeded the observed 2 μM f_u value obtained from undiluted plasma by ~110-, ~1300-, and ~2000-fold, respectively (Figure 5A). Similarly, after correcting these f_u values for plasma dilution by Eq. (14), the f_u values obtained using diluted plasma still exceeded the observed 2 μM undiluted plasma value by ~20 to ~120-fold (Figure 5B). When the effects of plasma dilution on C_{donor}/B_{max} ratio were accounted for by multiplying UCN-01 nominal concentrations by the plasma dilution factor (e.g., 2 μM in 5-fold diluted plasma = 10 μM), the dilution corrected f_u values obtained from 5-, 10-, and 20-fold diluted plasma were consistent with the expected values determined from UCN-01 plasma binding parameters (Figure 5C).

DMD Fast Forward. Published on February 2, 2018 as DOI: 10.1124/dmd.117.078915
This article has not been copyedited and formatted. The final version may differ from this version.

Venetoclax Dilution-Method Equilibrium Dialysis Results

Venetoclax plasma f_u value could not be determined using undiluted plasma at clinically relevant concentrations by equilibrium dialysis because receiver buffer concentrations were consistently below LLOQ. Using equilibrium dialysis dilution-method, venetoclax plasma f_u was measurable in 100-fold diluted plasma over a compound concentration range from 1 – 30 μM. No concentration dependency in f_u was observed over the concentration range tested. After correcting for plasma dilution, venetoclax undiluted-plasma f_u value was 0.000013 ± 0.0000064.

Discussion:

As early as the 1950s, dynamic dialysis was recognized as a superior approach compared to equilibrium dialysis for measuring f_u of compounds with high protein binding, but it has been used infrequently. This is likely due to its technical disadvantages (i.e., requirement for greater radiochemical purity, requirement to estimate P_{mem}, and the need for more sampling time-points to define the initial slope of compound appearance). Taking advantage of numerous technological advancements that have been made over the last ~20 years (improved bioanalytical methodologies, mass spectrometry, high-throughput 96-well equilibrium dialysis devices, kinetic modeling, etc.) we have tested and validated a modernized variation of dynamic dialysis (i.e., flux dialysis). Kinetic modeling, experimental data, and literature reference data supports flux dialysis as a method ideally suited for measuring f_u of compounds with extremely high protein binding, matrix instability, high non-specific binding and/or low bioanalytical sensitivity.

The kinetic model used to support the flux dialysis validation and to compare different dialysis-based protein binding methods is similar to a previously described equilibrium dialysis model (Di et al., 2012), but differs in three ways: 1) assumption that binding equilibrium is fast compared to the time scale of dialysis equilibrium ($k_{off} > k_{eq}$), thus using f_u and $K_{nsb,device}$ rather than k_{on} and k_{off} parameters, 2) saturable protein binding is accounted for through a 2-site binding equation rather than a single site, 3) allowance for dialysis against any matrix rather than conventional buffer only. Neither the Di et al. nor our model has an explicit algebraic solution for a traditional equilibrium dialysis time-course accounting for non-specific binding or compound degradation. However, the new kinetic model contains a simplified explicit solution assuming the compound degradation rate is equal in both compartments and that the compound's

affinity towards the matrix is greater than its affinity towards the device. This solution is the basis for determining f_u from both single and multiple time-point flux data. Another advantage of this new model structure and data treatment is that it is applicable to other dialysis or flux-based experimental approaches (e.g., permeability assays, microdialysis) and could allow more accurate calculations of initial flux rates, permeability or free drug concentrations (e.g., nanopartical/liposome formulation studies) than commonly used methods that assume initial sink or equilibrium conditions.

The estimated P_{mem} constant was similar across all compounds tested; allowing the average value of 75.2×10^{-6} cm/s to be used for all calculations (i.e., SF=3590 s). This value is highly consistent with the permeability through the unstirred water layer determined from 4 independently published Caco-2 studies (geomean $P_{app}^{max} = 73.6\times10^{-6}$ cm/s, range =37 – 200) (Avdeef et al., 2005) and the previously reported value for Spectra/Por dialysis tubing (~90×10^{-6} cm/s) (Ross, 1978). The similarity in P_{mem} constant from this study and literature indicate that the flux dialysis method could have been comparably validated using an independently determined P_{mem} constant from the literature (i.e., not using test compounds $f_{u,ref}$ values to calculate P_{mem}) and supports that compound permeability across the unstirred water layer appears to be similar across different in vitro systems and is not significantly influenced by compound properties. A constant P_{mem} value for all compounds is not unexpected if permeability across membrane unstirred water layer is the rate limiting step, since permeability across the unstirred water layer is compound independent assuming compound in solution behaves as an ideal solution (Wilke and Chang, 1955). The diffusion rate through the unstirred water layer however, is dependent on the unstirred water layer thickness and temperature (Wilke and Chang, 1955). The P_{mem} constant could differ depending on experimental conditions (e.g., temperature, shaking speed, membrane

thickness), so P_{mem} should be verified if different experimental conditions are used. Cited literature reports and our own work (data not shown) have shown that shaking speed above a certain minima has minimal influence on P_{mem}.

Accurate and precise (i.e., ≤ 2.5-fold of reported values; median inter-day %CV = 13%) f_u values for 14 compounds, 3 with previously unmeasurable f_u, were obtained at 1 µM concentration in undiluted plasma using the flux dialysis method. Given that 10 of the compounds had $f_u \leq 0.01$ (6 with $f_u < 0.001$), this degree of accuracy and precision is particularly striking as traditional protein binding methods are often validated using very few compounds with f_u <0.01 or only compare fraction bound values (e.g., fraction bound values 0.99 and 0.999 are similar, although f_u values differ 10-fold) (Banker et al., 2003; Ye et al., 2017).

Comparison to Traditional Equilibrium Dialysis Method

Equilibrium dialysis is a commonly used and often the preferred method to measure f_u; however, f_u results for compounds with high non-specific binding, matrix instability, and/or poor analytical sensitivity may be prone to inaccuracies. High non-specific binding to the dialysis device prolongs equilibrium time and can introduce errors if f_u results are determined before equilibrium is reached. Additionally, non-specific binding to labware may introduce errors in measuring the buffer concentrations, resulting in artificially low f_u values (Di et al., 2012). This is known to be problematic for lipophilic or poorly soluble compounds, such that when sampling buffer from dialysis device it is recommended that the buffer sample be directly added to the bioanalysis plate containing organic solvent and the pipette tip rinsed by mixing buffer sample and organic solvent together (Kalvass and Maurer, 2002; Di et al., 2012). Flux dialysis mitigates the effects of non-specific binding since compound is dialyzed against matrix, not buffer (Ross, 1978).

DMD Fast Forward. Published on February 2, 2018 as DOI: 10.1124/dmd.117.078915
This article has not been copyedited and formatted. The final version may differ from this version.

If a compound degrades during equilibrium dialysis the f_u results may be invalid since the free concentration in buffer and matrix can differ (Di et al., 2012). Depending on the cause of degradation, one or more of the following may overcome this: addition of chemical stabilizers/enzyme inhibitors, use of heat inactivated matrix, reducing temperature, and/or shielding from light. Alternatively, quicker methods such as ultrafiltration may be considered. Unfortunately, these "tricks" or alternative methods do not always work for compounds with challenging properties (Di et al., 2017). Flux modeling and experimental results (i.e., indomethacin) show that flux dialysis can be used for unstable compounds, as long as the rate of compound loss is equal in both dialysis compartments, as is the case when identical matrix is used on both sides.

Finally, the lowest discrete f_u value measurable by equilibrium dialysis is the buffer bioanalytical LLOQ divided by the total donor concentration. When the buffer concentration at equilibrium is below the LLOQ, only a qualified f_u can be reported (e.g., <0.01). In contrast, the flux dialysis receiver concentration is always higher than the corresponding free buffer concentrations from equilibrium dialysis since it will approach the total concentration of the donor matrix over time when the matrices are identical.

Comparison to Dilution Method

The dilution method (i.e., using diluted matrix) has been advocated to accelerate equilibrium time and measure f_u for compounds which are too highly bound to measure from undiluted plasma (Riccardi et al., 2015). The flux dialysis method was utilized to determine f_u values for venetoclax and UCN-01 in undiluted plasma, compounds which could previously only be measured using the dilution method. The venetoclax f_u showed no concentration dependence and was highly similar between the dilution method and flux dialysis method using undiluted

DMD Fast Forward. Published on February 2, 2018 as DOI: 10.1124/dmd.117.078915
This article has not been copyedited and formatted. The final version may differ from this version.

plasma. The similarity in f_u values between the two orthogonal methods provides confidence in the accuracy of the venetoclax f_u value and in the validity of the two methods when f_u is concentration independent.

In contrast, UCN-01 values showed large concentration dependence. Even after correcting for the dilution factor, UCN-01 f_u values from diluted plasma in the flux experiment were much larger than those determined from undiluted plasma in the same experiment. The f_u differences between diluted and undiluted plasma were not an artifact of the method, as diluted plasma f_u values from flux closely matched those previously published using equilibrium dialysis with identical compound concentration and plasma dilutions (Riccardi et al., 2015). The apparent f_u differences between the dilution method and undiluted plasma could be reconciled using a 2-site saturable binding equation which yielded binding parameters very similar to previously published values (Fuse et al., 1998). UCN-01 f_u differences obtained using diluted versus undiluted plasma can also be reconciled by a simpler novel approach of multiplying the nominal compound concentrations by the plasma dilution factor. For example, the dilution-corrected f_u value determined from 5-fold diluted plasma at 2 μM compound concentrations (i.e., 2 μM ×5 = 10 μM) is indistinguishable from the value determined from undiluted plasma at 10 μM compound concentration. Consequently, the dilution method offers no apparent advantage over simply using higher compound concentration in undiluted plasma and results generated using the dilution method may in fact be misleading for compounds with saturable binding, resulting in an overestimate of f_u if extrapolated to undiluted plasma. Furthermore, based on the dialysis kinetic model, matrix dilution does not meaningfully decrease equilibrium time compared to traditional equilibrium dialysis. Published equilibrium time-course for itraconazole, UCN-01, and amiodarone dialyzed in 5, 10 and 20-fold diluted plasma against buffer were all parallel at each

dilution level, demonstrating that time to equilibrium does not change with changing f_u or matrix dilution (Riccardi et al., 2015).

Comparison to Competition Method

Equilibrium dialysis of plasma against plasma has been used previously to determine relative differences in f_u values between different species (Clarke et al., 2008). The method is referred to as the competition method, in which the total concentration ratio between the two different plasmas at equilibrium represents the ratio of f_u between the two plasmas (i.e., equilibrium $plasma_1/plasma_2$ concentration ratio = $f_{u,plasma2}/f_{u,plasma1}$). Although measuring total concentration ratio can be technically less challenging than measuring free concentration from buffer, the competition method has two major disadvantages. First, the method does not allow measurements of actual discrete f_u values since only the f_u ratio is determined. Second, equilibrium time may take too long to be practical when $plasma_1$ and $plasma_2$ f_u values are small (Eriksson et al., 2005). The flux dialysis method exploits the same advantage of the competition method by measuring total plasma concentration rather than free buffer concentration, while adding the benefits of allowing for the calculation of actual f_u values and not requiring equilibrium to be reached.

Conclusion

The modern flux dialysis approach presented here mitigates the disadvantages of previous work using dynamic dialysis. This method utilizes modern mass spectrometry, high-throughput 96-well equilibrium dialysis devices and kinetic modeling to eliminate the requirement for greater radiochemical purity and reduces the burden associated with sampling multiple time-points under sink conditions. The determination of a constant P_{mem} has also alleviated the requirement of estimating individual P_{mem} values. The flux dialysis method enabled discrete measurements of

DMD Fast Forward. Published on February 2, 2018 as DOI: 10.1124/dmd.117.078915
This article has not been copyedited and formatted. The final version may differ from this version.

f_u for bedaquiline, lapatinib, pibrentasvir, UCN-01, and venetoclax, five compounds that exhibit extremely high protein binding for which discrete f_u values were not previously measurable from undiluted plasma at 1 μM compound concentration. Flux dialysis experiments conducted with identical matrix on both sides offers several advantages compared with other methods, such as increased receiver concentrations (to facilitate bioanalysis), reduced non-specific binding, valid f_u determination even when compound is unstable in matrix, no requirement for equilibrium (comparatively shorter dialysis times), and reduced problems associated with buffer samples (e.g., high nonspecific binding, absorption to surfaces, buffer standard curve). Therefore, flux dialysis is recommended as a valid and superior approach to equilibrium dialysis for compounds with high protein binding and other challenging properties.

Acknowledgments:

The authors kindly thank David M. Stresser for critically reading the manuscript and his editorial comments.

Authorship Contributions:

Participated in research design: *JCK, CP, GJ,*

Conducted experiments: *PS, XZ, LH*

Performed data analysis: *JCK, CP*

Wrote or contributed to the writing of the manuscript: *JCK, CP, GJ, MJMAN, VF, PS, XZ, LH*

References:

Avdeef A, Artursson P, Neuhoff S, Lazorova L, Grasjo J, and Tavelin S (2005) Caco-2 permeability of weakly basic drugs predicted with the double-sink PAMPA pKa(flux) method. *Eur J Pharm Sci* **24:**333-349.

Banker MJ, Clark TH, and Williams JA (2003) Development and validation of a 96-well equilibrium dialysis apparatus for measuring plasma protein binding. *J Pharm Sci* **92:**967-974.

Berry LM, Li C, and Zhao Z (2011) Species differences in distribution and prediction of human V(ss) from preclinical data. *Drug Metab Dispos* **39:**2103-2116.

Christensen LK (1959) A method for the determination of free, non-protein bound thyroxine in serum. *Scand J Clin Lab Invest* **11:**326-331.

Clarke HJ, Gregoire F, Ma F, Martin R, Zhao S, and Lavan BE (2008) Cross-species differential plasma protein binding of MBX-102/JNJ39659100: A novel PPAR-gamma agonist. *PPAR Res* **2008:**465715.

Di L, Breen C, Chambers R, Eckley ST, Fricke R, Ghosh A, Harradine P, Kalvass JC, Ho S, Lee CA, Marathe P, Perkins EJ, Qian M, Tse S, Yan Z, and Zamek-Gliszczynski MJ (2017) Industry perspective on contemporary protein-binding methodologies: Considerations for regulatory drug-drug interaction and related guidelines on highly bound drugs. *J Pharm Sci* **106:**3442-3452.

Di L, Umland JP, Trapa PE, and Maurer TS (2012) Impact of recovery on fraction unbound using equilibrium dialysis. *J Pharm Sci* **101:**1327-1335.

Eriksson MA, Gabrielsson J, and Nilsson LB (2005) Studies of drug binding to plasma proteins using a variant of equilibrium dialysis. *J Pharm Biomed Anal* **38:**381-389.

Fremstad D, Nilsen OG, Storstein L, Amlie J, and Jacobsen S (1979) Pharmacokinetics of quinidine related to plasma protein binding in man. *Eur J Clin Pharmacol* **15:**187-192.

Fuse E, Tanii H, Kurata N, Kobayashi H, Shimada Y, Tamura T, Sasaki Y, Tanigawara Y, Lush RD, Headlee D, Figg WD, Arbuck SG, Senderowicz AM, Sausville EA, Akinaga S, Kuwabara T, and

Kobayashi S (1998) Unpredicted clinical pharmacology of UCN-01 caused by specific binding to human alpha1-acid glycoprotein. *Cancer Res* **58:**3248-3253.

Indomethacin package insert. Iroko Pharmaceuticals, LLC, Philadelphia, PA; May 2016. http://www.accessdata.fda.gov/drugsatfda_docs/label/2016/018185s055s056lbl.pdf. Accessed Aug 12, 2016.

Kalvass JC and Maurer TS (2002) Influence of nonspecific brain and plasma binding on CNS exposure: implications for rational drug discovery. *Biopharm Drug Dispos* **23:**327-338.

Kalvass JC, Maurer TS, and Pollack GM (2007) Use of plasma and brain unbound fractions to assess the extent of brain distribution of 34 drugs: Comparison of unbound concentration ratios to in vivo p-glycoprotein efflux ratios. *Drug Metab Dispos* **35:**660-666.

Meyer MC and Guttman DE (1968) Novel method for studying protein binding. *J Pharm Sci* **57:**1627-1629.

Meyer MC and Guttman DE (1970a) Dynamic dialysis as a method for studying protein binding. I. Factors affecting the kinetics of dialysis through a cellophane membrane. *J Pharm Sci* **59:**33-38.

Meyer MC and Guttman DE (1970b) Dynamic dialysis as a method for studying protein binding. II. Evaluation of the method with a number of binding systems. *J Pharm Sci* **59:**39-48.

Motoya T, Thevanayagam LN, Blaschke TF, Au S, Stone JA, Jayewardene AL, Chi J, and Aweeka FT (2006) Characterization of nelfinavir binding to plasma proteins and the lack of drug displacement interactions. *HIV Med* **7:**122-128.

Riccardi K, Cawley S, Yates PD, Chang C, Funk C, Niosi M, Lin J, and Di L (2015) Plasma protein binding of challenging compounds. *J Pharm Sci* **104:**2627-2636.

Ronfeld RA, Tremaine LM, and Wilner KD (1997) Pharmacokinetics of sertraline and its N-demethyl metabolite in elderly and young male and female volunteers. *Clin Pharmacokinet* **32 Suppl 1:**22-30.

Ross HA (1978) A dialysis rate method for the measurement of free iodothyronine and steroid hormones in blood. *Experientia* **34:**538-539.

U.S. FDA. Center for Drug Evaluation and Research. Sirturo NDA 204384 Clinical Pharmacology and Biopharmaceutics Review, Section 2.2.5.4, December 10, 2012. http://www.accessdata.fda.gov/drugsatfda_docs/nda/2012/204384Orig1s000ClinPharmR.pdf. Accessed October 26, 2016.

U.S. FDA. Center for Drug Evaluation and Research. Tykerb NDA 22-059 Clinical Pharmacology and Biopharmaceutics Review, Section 2.2.5.4, January 24, 2007. http://www.accessdata.fda.gov/drugsatfda_docs/nda/2007/022059s000_ClinPharmR.pdf. Accessed October 26, 2016.

Wan H and Rehngren M (2006) High-throughput screening of protein binding by equilibrium dialysis combined with liquid chromatography and mass spectrometry. *J Chromatogr A* **1102:**125-134.

Wilke C and Chang P (1955) Correlation of diffusion coefficients in dilute solutions. *AIChE Journal* **1:**264-270.

Ye Z, Zetterberg C, and Gao H (2017) Automation of plasma protein binding assay using rapid equilibrium dialysis device and Tecan workstation. *J Pharm Biomed Anal* **140:**210-214.

Footnotes:

The design, study conduct, and financial support for this study were provided by AbbVie. AbbVie participated in the interpretation of data, writing, review, and approval of publication. All authors are current employees of AbbVie.

DMD Fast Forward. Published on February 2, 2018 as DOI: 10.1124/dmd.117.078915
This article has not been copyedited and formatted. The final version may differ from this version.

Legends for Figures:

Figure 1. Flux dialysis kinetic model. The model is comprised of donor and receiver matrix compartments separated by a semipermeable membrane. The receiver compartment is always defined as the compartment with the lowest matrix unbound compound concentration. X_0 denotes compound mass at time zero, V denotes the compartment volumes, A denotes the membrane surface area, and P_{mem} denotes the unbound compound dialysis-membrane permeability. C denotes the total compound concentrations, f_u denotes the compound matrix unbound fractions, k_{loss} the compound first-order rates of irreversible loss (e.g., degradation or covalent binding), and $K_{nsb,device}$ denotes the non-specific compound binding potentials to the dialysis device.

Figure 2. Representative receiver/donor ratio versus time data from a single flux dialysis experiment. Symbols represent compound receiver/donor matrix concentration ratio determined in triplicate at different time-points over a 96 hour dialysis period. Lines represent non-linear fit of $R=R_{eq}\cdot(1-e^{-k\cdot t})$ to receiver/donor concentration vs time data. During the dialysis period, purchased human plasma spiked with 1 μM compound (donor matrix) was dialyzed against compound-free purchased human plasma (receiver matrix). Aliquots of donor and receiver matrix (10 μL) were sampled from each dialysis well at 0.25, 0.5, 2, 4, 24, 48, and 96 hour and compound concentration determined by HPLC-MS/MS.

Figure 3. Unbound fraction determined by flux dialysis versus reported values determined from other methods. Black solid and dashed lines represent the line of unity and ±2.5-fold unity, respectively. Dotted line represents line from log-log orthogonal regression analysis. Flux dialysis f_u value for each compound was determined from product each compound's average

DMD Fast Forward. Published on February 2, 2018 as DOI: 10.1124/dmd.117.078915
This article has not been copyedited and formatted. The final version may differ from this version.

R_{slope} and SF (3590 s) according to Eq. (8) in method section. Reported f_u values were obtained from the literature or internal AbbVie reports (glecaprevir and venetoclax).

Figure 4. Indomethacin receiver/donor ratio versus time (A), indomethacin flux dialysis recovery versus time (B), and concordance between R_{slope} determined from single time-point vs fitted time-course (C). Data represent 3 individual experiments run in duplicates on 3 separate days with each inter-day experiment denoted with a different color and shaped symbol. Lines in panel A represent non-linear power fit function to the % recovery vs time data from indomethacin flux dialysis experiments. Lines in panel B represent non-linear fit of $R=R_{eq}\cdot(1-e^{-k\cdot t})$ to indomethacin receiver/donor concentration vs time data. Solid line in panel C represents the unity line (1.0) and dashed lines represent ±2-fold line of unity (0.5 and 2). R_{slope} (1-pt) is the R_{slope} value calculated at each time-point using only data from that single time-point and Eq. (7). R_{slope} (fitted) is the R_{slope} value determined from the fit of Eq. (5) to the entire receiver/donor concentration time-course.

Figure 5. UCN-01 observed (symbols) and model-fitted (lines) f_u values obtained at various UCN-01 concentrations and plasma dilutions (○ undiluted, ○ 5-, ○ 10-, or ○ 20-fold dilution). **"**Measured" f_u values not corrected for plasma dilution **(A)**, calculated "undiluted" plasma f_u values corrected by Eq, (14) for the effect of plasma dilution **(B)**, and calculated "undiluted" plasma f_u values corrected by Eq, (14) and by multiplying UCN-01 nominal concentrations by the plasma dilution factor (e.g., 2 µM in 5-fold diluted plasma = 10 µM) to account for the effect of plasma dilution on C_{donor}/B_{max} ratio **(C)**. Lines represent simultaneous fit of the 2-site saturable binding equation, Eq. (16), to all UCN-01 f_u data.

DMD Fast Forward. Published on February 2, 2018 as DOI: 10.1124/dmd.117.078915
This article has not been copyedited and formatted. The final version may differ from this version.

Tables:

Table 1. MS/MS instrument setting

Compound	MRM	DP	CE	Ionization mode
amiodarone	646 → 100	94	50	Positive
bedaquiline	555 → 58	50	75	Positive
glecaprevir	840 → 684	100	35	Positive
glyburide	494 → 369	54	22	Positive
indomethacin	358 → 139	59	37	Positive
imipramine	281 → 86	40	25	Positive
itraconazole	705 → 392	83	52	Positive
lapatinib	581 → 365	107	53	Positive
nelfinavir	569 → 330	59	48	Positive
pibrentasvir	557* → 146	200	30	Positive
quinidine	325 → 172	86	50	Positive
sertraline	306 → 159	63	41	Positive
7-hydroxystaurosporine (UCN-01)	483 → 130	100	25	Positive
venetoclax	869 → 636	20	40	Positive

MRM (multiple reaction monitoring); DP (declustering potential); CE (collision energy)

*Doubled charged ion

DMD Fast Forward. Published on February 2, 2018 as DOI: 10.1124/dmd.117.078915
This article has not been copyedited and formatted. The final version may differ from this version.

Table 2. R_{slope}, unbound fraction from flux dialysis, and unbound fraction reference values

Compound	R_{slope} (%CV) ($s^{-1} \times 10^{-6}$)	Flux dialysis f_u [b]	Reported f_u (reference)
imipramine	38.9 (23%)	0.14	0.13 (Berry et al., 2011)
quinidine	31.1 (8%)[a]	0.11	0.22 (Fremstad et al., 1979)
sertraline	9.72 (8%)[a]	0.035	0.016 (Ronfeld et al., 1997)
glecaprevir	6.67 (21%)	0.024	0.025 (AbbVie data on file)
indomethacin	2.61 (13%)	0.0094	0.010 (Indomethacin package insert)
nelfinavir	0.778 (7%)[a]	0.0028	0.0042 (Motoya et al., 2006)
itraconazole	0.583 (5%)	0.0021	0.0021 (Riccardi et al., 2015)
glyburide	0.317 (6%)	0.0011	0.0010 (Wan and Rehngren, 2006)
lapatinib	0.211 (10%)	0.00076	< 0.011 (U.S. FDA)
UCN-01	0.0247 (1%)	0.000089	0.000073[c] (Fuse et al., 1998)
pibrentasvir	0.0172 (33%)	0.000062	< 0.0001 (AbbVie data on file)
amiodarone	0.0158 (8%)	0.000057	0.00014 (Riccardi et al., 2015)
bedaquiline	0.00806 (15%)	0.000029	< 0.0001 (U.S. FDA)
venetoclax	0.00333 (32%)	0.000012	0.000013 (AbbVie data on file)

%CV = inter-assay %CV calculated from experiments conducted on separated days (n= 2-5experiments); %CV values for flux dialysis f_u are identical to R_{slope} %CV, therefore are not reported separately

a = intra-assay %CV calculated from a single experiment run in triplicate

b = Calculated as $R_{slope} \times 3590$ s

c = f_u value calculated from published B_{max} and K_D values (i.e., $f_u = K_D/(K_D+B_{max}) = 0.0012/(0.0012+16.4) = 0.000073$)

DMD Fast Forward. Published on February 2, 2018 as DOI: 10.1124/dmd.117.078915
This article has not been copyedited and formatted. The final version may differ from this version.

Table 3. Compound unbound dialysis membrane permeability (P_{mem}) and physiochemical properties*

Compound	P_{mem} (%CV) ($cm/s \times 10^{-6}$)	Mol. wt.	pKa (most acidic)	pKa (most basic)	Molar intrinsic solubility (μM)	LogP	LogD 7.0	Polar surface area (A^2)
amiodarone	30.5 (8%)	645.31		9.37	0.076	7.815	5.51	42.7
bedaquiline	n.c.	555.5	13.05	9.31	0.032	7.712	5.8	45.6
glecaprevir	72.1 (21%)	838.87	4.46	-1.38	3.5	-0.88	-0.7	204
glyburide	85.7 (6%)	494	5.11	-1.63	7.9	3.076	1.22	122
imipramine	80.9 (23%)	280.41		9.49	45	4.355	2	6.48
indomethacin	70.5 (13%)	357.79	3.96		17	4.251	1.29	68.5
itraconazole	75.0 (5%)	705.63		6.47	0.14	4.995	4.86	101
lapatinib	n.c.	581.06		6.34	0.0029	6.302	6.21	115
nelfinavir	50.1 (7%)[a]	567.78	9.58	6.21	1.5	7.278	7.25	127
pibrentasvir	n.c.	1113.18	9.76	6.33	0.088	5.812	5.73	200
quinidine	38.2 (8%)[a]	324.42	12.8	9.28	450	2.823	0.62	45.6
sertraline	164 (8%)[a]	306.23		9.47	17	5.079	2.7	12
UCN-01	91.4 (1%)	482.53	12.25	8.93	0.18	4.983	3.07	89.7
venetoclax	69.2 (32%)	868.44	4.09	8.34	0.0072	8.051	3.97	183

*Physiochemical properties calculated using Advanced Chemistry Development (ACD/Labs) Software V11.02 (© 1994-2017 ACD/Labs)

n.c.= not calculated due to lack of reference f_u

%CV = inter-assay %CV calculated from experiments conducted on separated days (n= 2-5 experiments);

a = intra-assay %CV calculated from single experiment run in triplicate

Average $P_{mem} \pm SD = 75 \pm 35 \times 10^{-6}$ cm/s^2

Table 4. Advantages and disadvantages of determining unbound fraction by different dialysis methods

	Eq. Dialysis Method (matrix vs buffer)	Eq. Dilution Method (diluted-matrix vs buffer)	Eq. Competition Method ($matrix_1$ vs $matrix_2$)	Flux Dialysis Method (matrix vs matrix)
Minimal dialysis time	**(-) Establishment of equilibrium,** (HTDialysis ≤ 4 h assuming minimal non-specific binding)	**(-) Establishment of equilibrium,** (HTDialysis ≤ 4 h assuming minimal non-specific binding)	**(-) Establishment equilibrium,** (hours, days, weeks or months depending on f_u)	**(+) Receiver conc >> LLOQ,** (always faster than equilibrium dialysis assuming same LLOQ
Impact of Device Non-Specific Binding	**(-) Increased time to equilibrium,** (although no impact on f_u)	**(-) Increased time to equilibrium,** (although no impact on f_u)	**(+) Non-specific binding is minimized**	**(+) Non-specific binding is minimized**
Impact of Compound Matrix Instability	**(-) Invalid f_u**	**(-) Invalid f_u**	**(-) Invalid f_u** if degradation rate is different between $matrix_1$ and $matrix_2$	**(+) No impact on f_u**
Sample Composition	**(-) Matrix and buffer,** 2 standard curves or sample blanking/matching require; Additional GLP validation and lower LLOQ may be required	**(-) Matrix and buffer,** 2 standard curves or sample blanking/matching require; Additional GLP validation and lower LLOQ may be required	**(-) $Matrix_1$ and $matrix_2$,** 2 standard curves or sample blanking/matching require; Additional GLP validation may be required	**(+) All samples identical matrix,** single standard curve ; pre-existing GLP assay likely can be used
LLOQ Requirement	**(-) LLOQ ≤ free buffer**	**(-) LLOQ ≤ free buffer,** although free buffer increases roughly proportional with dilution factor	**(+) LLOQ ≤ initial matrix conc** assuming similar f_u between $martix_1$ and $matrix_2$	**(+) LLOQ ≤ ½ initial donor conc**
Additional Advantage/ Disadvantages	**(+) Most commonly used dialysis method**	**(-) Risk for saturating protein binding;** **(-) Dilution does not reduce equilibrium time**	**(-) Discrete f_u not determined**, only f_u ratio between matrix1 and matrix2	**(-) Unconventional time-point(s) and data may require non-linear curve fitting**

(+) and (-) symbols indicated attributes of relative advantage or disadvantage, respectively

DMD Fast Forward. Published on February 2, 2018 as DOI: 10.1124/dmd.117.078915
This article has not been copyedited and formatted. The final version may differ from this version.

Appendix:

Appendix A

The system of differential equations corresponding to the experimental setup in Figure 1, and the solutions to these equations in various cases of interest are presented below.

Let A (cm^2) denote the surface area of the membrane and P_{mem} (mL/s/cm^2) the unbound membrane permeability to a specific compound. The compartment volumes, V (mL), fractions unbound, f_u, total concentrations, C (μM), and first-order rates of irreversible loss (e.g., due to degradation or covalent binding), k_{loss} (1/s), are all specified with the appropriate compartment subscript (donor or receiver). The general system is given by:

$$\frac{dC_{donor}}{dt} = \frac{P_{mem} \times A}{V_{donor}}\left(f_{u,receiver} \times C_{receiver} - f_{u,donor} \times C_{donor}\right) - k_{loss,donor} \times C_{donor} \quad \text{(A1)}$$

$$\frac{dC_{receiver}}{dt} = \frac{P_{mem} \times A}{V_{receiver}}\left(f_{u,donor} \times C_{donor} - f_{u,receiver} \times C_{receiver}\right) - k_{loss,receiver} \times C_{receiver} \quad \text{(A2)}$$

Introducing permeability-surface area products per unit volume $\mu = P_{mem} \times A/V$, the above equations can be rewritten as

$$\frac{dC_{donor}}{dt} = \mu_{donor}\left(f_{u,receiver} \times C_{receiver} - f_{u,donor} \times C_{donor}\right) - k_{loss,donor} \times C_{donor} \quad \text{(A3)}$$

$$\frac{dC_{receiver}}{dt} = \mu_{receiver}\left(f_{u,donor} \times C_{donor} - f_{u,receiver} \times C_{receiver}\right) \quad \text{(A4)}$$

DMD Fast Forward. Published on February 2, 2018 as DOI: 10.1124/dmd.117.078915
This article has not been copyedited and formatted. The final version may differ from this version.

$$-k_{loss,receiver} \times C_{receiver}$$

Subject to the initial conditions

$$C_{donor} = \frac{X_0}{V_{donor}}, C_{receiver} = 0,$$

where X_0 is the amount of compound added to the donor compartment at time=0, analytical solutions for the concentration-time profiles exist and are of the form

$$C_{donor}(t) = \frac{X_0}{V_{donor}}\left(\frac{1}{r_2 - r_1}\right)[(r_2 - \alpha_{donor})e^{-r_1 t} + (\alpha_{donor} - r_1) \times e^{-r_2 t}] \quad \text{(A5)}$$

$$C_{receiver}(t) = \frac{X_0}{V_{receiver}}\left(\frac{f_{u,donor}\mu_{donor}}{r_2 - r_1}\right)(e^{-r_1 t} - e^{-r_2 t}) \quad \text{(A6)}$$

where

$$r_{1,2} = \left(\alpha_{donor} + \alpha_{receiver} \mp \sqrt{(\alpha_{donor} - \alpha_{receiver})^2 + 4 f_{u,donor} f_{u,receiver} \mu_{donor} \mu_{receiver}}\right)/2$$

$$\alpha_{compartment} = k_{loss,compartment} + f_{u,compartment} \times \mu_{compartment}.$$

These solutions simplify to a manageable form when the assumption of equal loss rates in both compartments is made, i.e. $k_{loss,receiver} = k_{loss,donor} = k_{loss}$. In this case

$$C_{donor}(t) = \frac{X_0}{V_{donor}} \times \frac{1}{(1+\beta)} \times e^{-k_{loss} t} \times \left(1 + \beta e^{-k_{eq} t}\right) \quad \text{(A7)}$$

$$C_{receiver}(t) = \frac{X_0}{V_{receiver}} \times \frac{\beta}{(1+\beta)} \times e^{-k_{loss} t} \times \left(1 - e^{-k_{eq} t}\right) \quad \text{(A8)}$$

where

$$\beta = \frac{f_{u,donor}}{f_{u,receiver}} \times \frac{V_{receiver}}{V_{donor}}$$

DMD Fast Forward. Published on February 2, 2018 as DOI: 10.1124/dmd.117.078915
This article has not been copyedited and formatted. The final version may differ from this version.

and k_{eq} is the equilbrative rate constant given by:

$$k_{eq} = (P_{mem} \times A)\left(\frac{f_{u,donor}}{V_{donor}} + \frac{f_{u,receiver}}{V_{receiver}}\right) \qquad \text{(A9)}$$

The total amount of compound in the system, A_{total}, is not conserved in the system when loss is present. In this simplifed case, the total amount of compoound exponentially decays and is described by the expression

$$A_{total} = (C_{receiver} \times V_{receiver}) + (C_{donor} \times V_{donor}) = X_0 \times e^{-k_{loss}t}$$

The ratio of concentrations,

$$R = \frac{C_{receiver}(t)}{C_{donor}(t)}$$

from equations (A7) and (A8) yields

$$R = \frac{f_{u,donor}}{f_{u,receiver}} \times \frac{\left(1 - e^{-k_{eq}t}\right)}{\left(1 + \beta e^{-k_{eq}t}\right)} \qquad \text{(A10)}$$

and is equal to $f_{u,donor}/f_{u,receiver}$ at steady state (time = infinity). This concentration ratio is denoted by

$R_{eq} = \frac{f_{u,donor}}{f_{u,receiver}}$.

Note the absence of any impact of k_{loss} in the equation for R above in Eq. (A10). This analysis indicates that even in the presence of loss that so long as the loss rates in both compartments are equal, then there is no effect of loss on the concentration ratio.

Assuming equal fraction unbound in both compartments, i.e. $f_{u,receiver} = f_{u,donor} = f_u$, or equivalently, $R_{eq} = 1$,

DMD Fast Forward. Published on February 2, 2018 as DOI: 10.1124/dmd.117.078915
This article has not been copyedited and formatted. The final version may differ from this version.

$$C_{donor}(t) = \frac{X_0}{V_{receiver} + V_{donor}} \times e^{-k_{loss}t} \times \left(1 + \frac{V_{receiver}}{V_{donor}} e^{-f_u(\mu_{donor}+\mu_{receiver})t}\right) \quad \text{(A11)}$$

$$C_{receiver}(t) = \frac{X_0}{V_{receiver} + V_{donor}} \times e^{-k_{loss}t} \times \left(1 - e^{-f_u(\mu_{donor}+\mu_{receiver})t}\right) \quad \text{(A12)}$$

$$R = \frac{1 - e^{-f_u(\mu_{donor}+\mu_{receiver})t}}{1 + \frac{V_{receiver}}{V_{donor}} e^{-f_u(\mu_{donor}+\mu_{receiver})t}}. \quad \text{(A13)}$$

If we further assume that $V_{receiver} = V_{donor} = V$ then we obtain the expression

$$R = \frac{1 - e^{-2f_u\mu t}}{1 + e^{-2f_u\mu t}}, \quad \text{(A14)}$$

with a common permeability parameter for each compartment $\mu = P_{mem} \times A/V$. This expression is equilavent to $R = \tanh(f_u\mu t)$.

If we also consider the case where there is no loss in either compartment, i.e. $k_{loss,receiver} = k_{loss,donor} = 0$, subject to the same initial conditions yields donor and receiver concentration-time equations:

$$C_{donor}(t) = \frac{X_0}{V_{donor}} \times \frac{1}{(1+\beta)}\left(1 + \beta e^{-k_{eq}t}\right) \quad \text{(A15)}$$

$$C_{receiver}(t) = \frac{X_0}{V_{receiver}} \times \frac{\beta}{(1+\beta)}\left(1 - e^{-k_{eq}t}\right) \quad \text{(A16)}$$

These equations satisfy the mass conservation equation:

$$A_{total} = (C_{receiver} \times V_{receiver}) + (C_{donor} \times V_{donor}) = X_0,$$

at all times.

The ratio of concentrations from equations (A15) and (A16) yields exactly the same expression as that achieved when assuming equal loss rates given in (A10).

In the case where the concentration ratio is given in Eq. (A10), then the approximation to the function about time t=0, is given by

$$R_0 \approx \frac{f_{u,donor} \times P_{mem} \times A}{V_{receiver}} t$$

and thus the slope near time=0 is given by

$$R_{slope} = \frac{f_{u,donor} \times P_{mem} \times A}{V_{receiver}}, \qquad \text{(A17)}$$

which is identical to the expression obtained by assuming initial sink conditions (Eq (4)).

In order to account for non-specific device binding, we will assume that the process is instantaneously in equilibrium, similar to the assumption made for protein binding. In this case, we will need to differentiate between the fraction unbound to the device, $f_{u,device}$, the fraction unbound to protein, $f_{u,matrix}$, which is the quantity of interest, and the total composite fraction unbound in the presence of both binding events, f_u.

If both non-specific device binding and protein binding processes are in equilibrium then the observed composite fraction unbound in each compartment is given by

DMD Fast Forward. Published on February 2, 2018 as DOI: 10.1124/dmd.117.078915
This article has not been copyedited and formatted. The final version may differ from this version.

$$f_u = \frac{1}{1 + \left(\frac{1}{f_{u,matrix}} - 1\right) + \left(\frac{1}{f_{u,device}} - 1\right)} \qquad \text{(A18)}$$

where

$$f_{u,device} = \frac{1}{K_{nsb,device} + 1}$$

where $K_{nsb,device} (= B_{max,NS}/K_{D,NS})$ is the nonspecific binding potential to the device under the assumption that $K_{D,NS} \gg C_u$. Inserting this expression into the one above gives

$$f_u = \frac{1}{\frac{1}{f_{u,matrix}} + K_{nsb,device}} \qquad \text{(A19)}$$

If nonspecific binding is negligible relative to matrix binding, i.e. $1/K_{nsb,device} \gg f_{u,matrix}$, then $f_u = f_{u,matrix}$. However, if nonspecific binding is not negligible then the expression for f_u in Eq. (A19) must be substituted into equations (A1)-(A17) given above. Specifically the expression for the concentration ratio is

$$R = R_{eq} \times \frac{\left(1 - e^{-k_{eq}t}\right)}{\left(1 + \beta e^{-k_{eq}t}\right)},$$

where

$$k_{eq} = (P_{mem} \times A)\left(\frac{1}{V_{donor}\left(\frac{1}{f_{u,donor}} + K_{nsb,device}\right)} + \frac{1}{V_{receiver}\left(\frac{1}{f_{u,receiver}} + K_{nsb,device}\right)}\right).$$

(A20)

Notable ramifications of nonspecific binding include the necessity of correcting the f_u obtained from the initial slope given by Eq. (A17) in order to arrive at the desired $f_{u,matrix}$. This would require knowledge of nonspecific binding parameters and utilization of the rearranged form of Eq. (A19)

$$f_{u,matrix} = \frac{1}{\frac{1}{f_u} - K_{nsb,device}} \qquad \text{(A21)}$$

From Eq. (A20) we observe that in the presence of non-specific binding, the time to equilibrium is extended by a factor of $(1 + K_{nsb,device} \times f_{u,matrix})$.

DMD Fast Forward. Published on February 2, 2018 as DOI: 10.1124/dmd.117.078915
This article has not been copyedited and formatted. The final version may differ from this version.

Appendix B: Fraction unbound in the presence of saturable and non-saturable binding

In the presence of saturable (S) and non-saturable (NS) binding sites, the bound concentration at equilibrium is given by the equation

$$C_b = \frac{B_{max} \times C_u}{K_D + C_u} + K_{nsb} \times C_u$$

where B_{max} and K_D are the binding capacity and equilibrium dissociation constant of the specific binding site, and $K_{nsb}(= B_{max,NS}/K_{D,NS})$ is the nonspecific binding potential. The total concentration, $C = C_b + C_u$, is then

$$C = \frac{B_{max} \times C_u}{K_D + C_u} + K_{nsb} \times C_u + C_u.$$

Rearranging yields

$$(1 + K_{nsb})C_u^2 + (B_{max} + K_D(1 + K_{nsb}) - C) \times C_u - K_D \times C = 0$$

and solving for C_u gives

$$C_u = \frac{C - \left(B_{max} + K_D(1 + K_{nsb})\right) + \sqrt{\left(C - \left(B_{max} + K_D(1 + K_{nsb})\right)\right)^2 + 4K_D(1 + K_{nsb})C}}{2(1 + K_{nsb})}.$$

The fraction unbound, f_u, is then given by the ratio of this unbound concentration to the total concentration

$$f_u = \frac{C - \left(B_{max} + K_D(1 + K_{nsb})\right) + \sqrt{\left(C - \left(B_{max} + K_D(1 + K_{nsb})\right)\right)^2 + 4K_D(1 + K_{nsb})C}}{2(1 + K_{nsb})C}.$$

DMD Fast Forward. Published on February 2, 2018 as DOI: 10.1124/dmd.117.078915
This article has not been copyedited and formatted. The final version may differ from this version.

Figure 1.

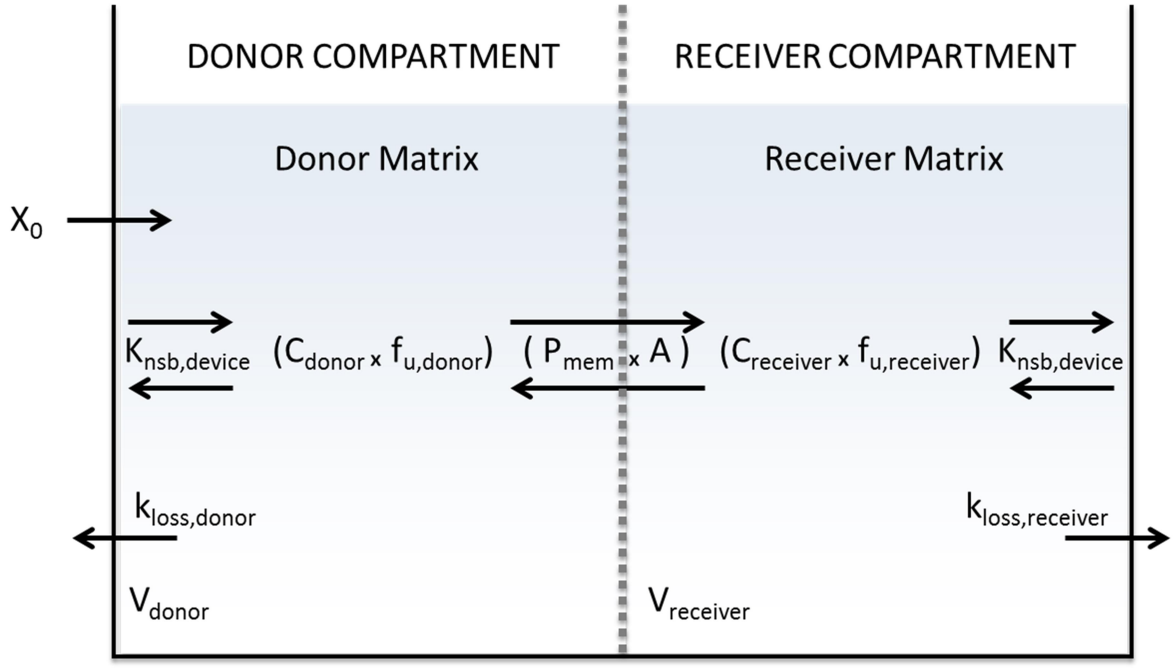

DMD Fast Forward. Published on February 2, 2018 as DOI: 10.1124/dmd.117.078915
This article has not been copyedited and formatted. The final version may differ from this version.

Figure 2.

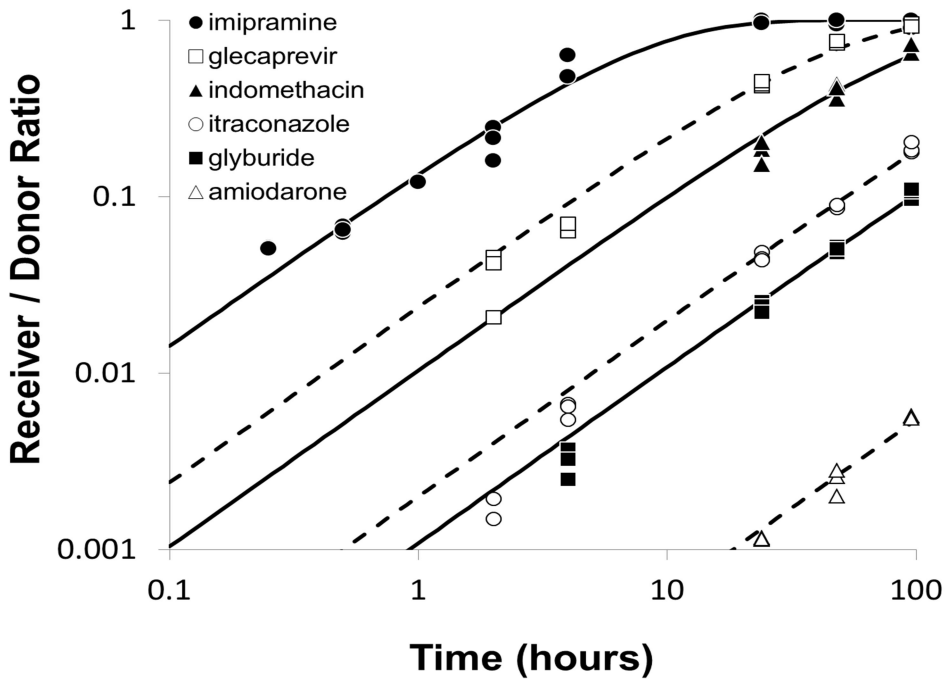

DMD Fast Forward. Published on February 2, 2018 as DOI: 10.1124/dmd.117.078915
This article has not been copyedited and formatted. The final version may differ from this version.

Figure 3.

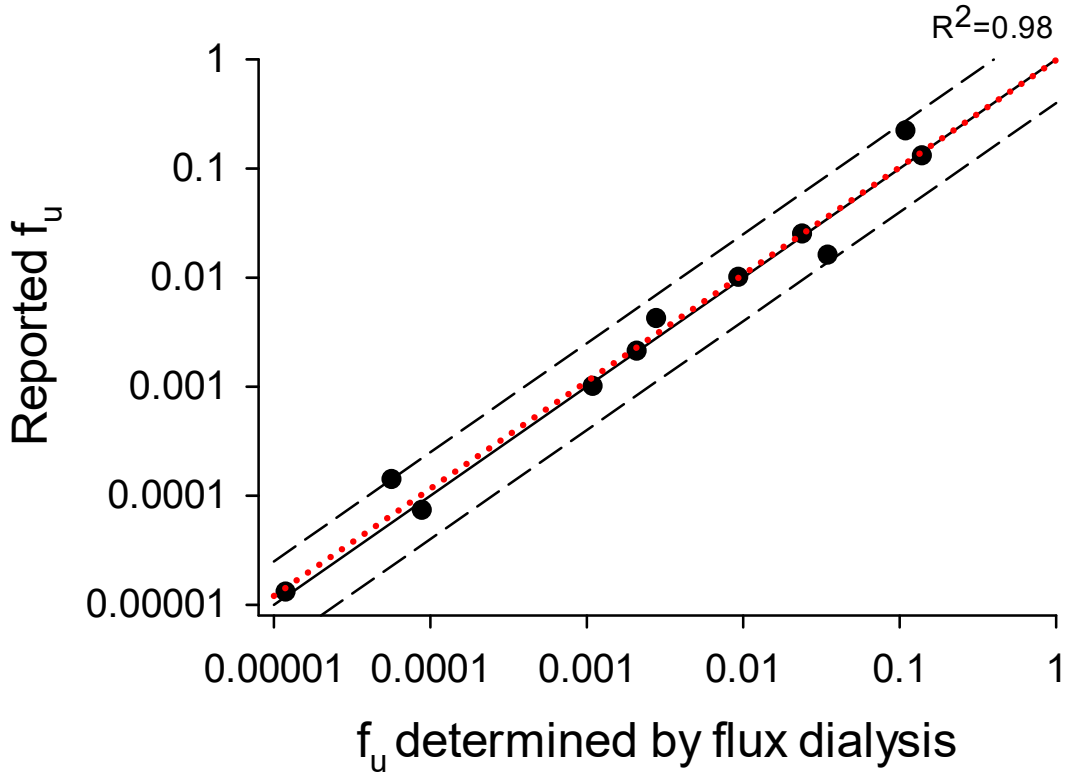

DMD Fast Forward. Published on February 2, 2018 as DOI: 10.1124/dmd.117.078915
This article has not been copyedited and formatted. The final version may differ from this version.

Figure 4.

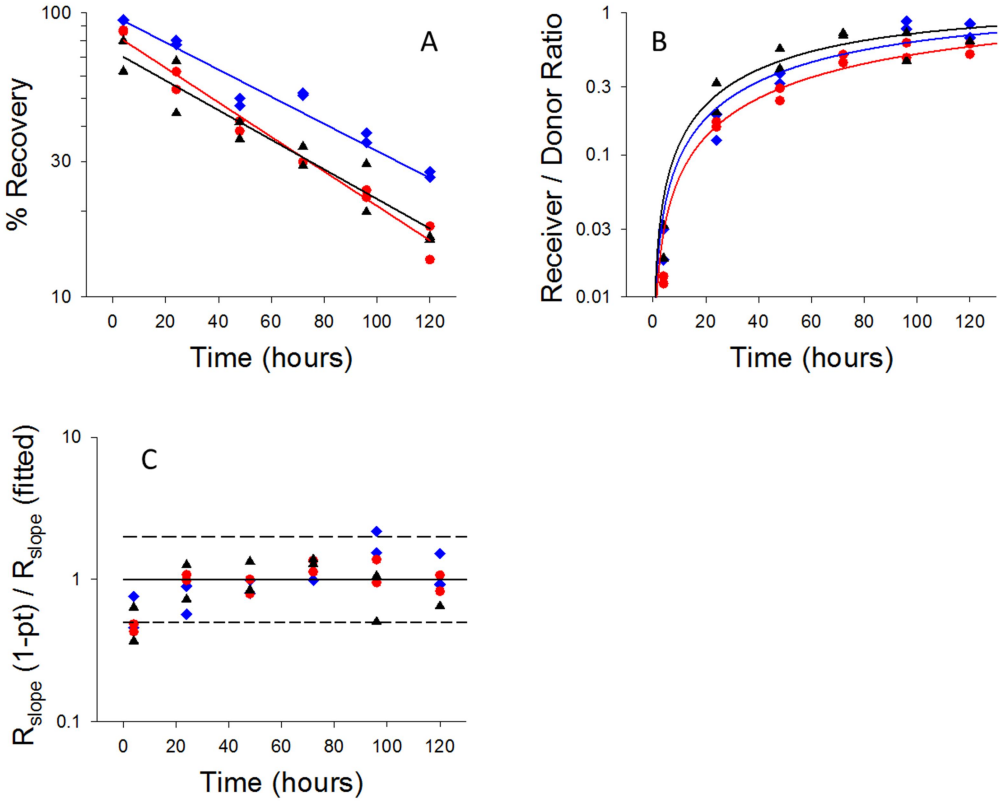

DMD Fast Forward. Published on February 2, 2018 as DOI: 10.1124/dmd.117.078915
This article has not been copyedited and formatted. The final version may differ from this version.

Figure 5.